

Dewetting Inhibition and Interfacial Structures of Silsesquioxane-terminated Polystyrene Thin Films

Kyota MIYAMOTO,¹ Nao HOSAKA,¹ Motoyasu KOBAYASHI,² Hideyuki OTSUKA,^{1,2}
Norifumi YAMADA,³ Naoya TORIKAI,³ and Atsushi TAKAHARA^{1,2,†}

¹Graduate School of Engineering, Kyushu University, 744 Motoooka, Nishi-ku, Fukuoka 819-0395, Japan

²Institute for Materials Chemistry and Engineering, Kyushu University,
744 Motoooka, Nishi-ku, Fukuoka 819-0395, Japan

³Neutron Science Laboratory, Institute of Materials Structure Science,
High Energy Accelerator Research Organization, 1-1 Oho, Tsukuba 305-0801, Japan

(Received June 5, 2007; Accepted August 2, 2007; Published October 10, 2007)

ABSTRACT: Polyhedral oligomeric silsesquioxane (POSS)-terminated polystyrene (PS-POSS) was prepared by nitroxide-mediated radical polymerization of styrene with POSS-containing initiator, and the thermal stability of PS-POSS thin films was investigated. Rheological measurement of PS-POSS revealed that the rheological properties were profoundly affected by the presence of POSS end groups in low molecular weight region ($M_n \approx 2000$), while those were nearly unaffected in high molecular weight region ($M_n \approx 40000$). However, the introduction of POSS as a PS end group can actually stabilize PS thin films against dewetting in a range of the molecular weight used in this study. Neutron reflectivity measurement of deuterated PS-POSS thin film revealed that the POSS moieties of PS-POSS formed enrichment layer at the interfaces of the film. The segregation of the POSS end group at the film–substrate interface, which can modify the interface by tethering the PS chains at the interface, seems to be an important factor in the dewetting inhibition effect. [doi:10.1295/polymj.PJ2007067]

KEY WORDS Polyhedral Oligomeric Silsesquioxanes / Polymer Thin Film / Dewetting /
Rheological Properties / Neutron Reflectivity /

Polymer thin films have numerous technological applications which require the presence of a homogeneous film. However, producing stable films is problematic since the polymer thin films tend to dewet from the substrates.¹ Various approaches have been adopted to stabilize these films against dewetting including a modification of the substrate roughness or chemistry by irradiation,² grafting chains onto the substrate,³ the introduction of specialized end groups onto the polymer with a high affinity for the inorganic substrate,⁴ and the use of functional additives.⁵

Our previous study showed that the addition of polyhedral oligomeric silsesquioxanes (POSS) as a nanofiller is efficient for the stabilization of polymer thin film.⁶ POSS, of which the most common octameric structure is characterized by the formula of $R_8Si_8O_{12}$, is one of nanosized materials with a silica core and organic groups on the surface providing a high compatibility with organic polymers. POSS-containing nanostructured chemicals can be thought as the smallest possible particles of silica. The salient feature of this nanosized building block is the ability to functionalize the silicon corners with a variety of organic substituents. POSS cages can be incorporated

into polymer systems *via* polymerization, grafting, and blending by introducing the specific functionalities. By such hybridization, properties superior to the organic materials alone are realized, offering exciting possibilities for the development of new materials.^{7–9}

The blending of octacyclopentyl-POSS (CpPOSS) with the polystyrene (PS) thin films led to an inhibition of dewetting in the films. However, due to the low affinity of CpPOSS with PS, the film surface was roughened by the aggregation of CpPOSS in the films after annealing treatment.¹⁰ To improve the dispersibility of POSS into polymer thin films, the authors synthesized the POSS-terminated PS (PS-POSS), and added the small amount of PS-POSS into PS thin films as a nanofiller. In that case, the enhancement of the dispersibility of POSS cages into PS films and the thermal stabilization of the films was demonstrated.¹¹

The present work is focused on the thermal stability of pure PS-POSS thin films. POSS plays the role of an end group of PS chains but not a nanofiller. PS-POSS was prepared by nitroxide-mediated radical polymerization (NMRP)¹² of styrene with POSS-containing initiator having 2,2,6,6-tetramethylpiperidine-1-oxyl

[†]To whom correspondence should be addressed (Tel: +81-92-802-2517, Fax: +81-92-802-2518, E-mail: takahara@cstf.kyushu-u.ac.jp).

(TEMPO)-based alkoxyamine unit. The rheological and thermal properties of the polymer chains with a nanoparticle as an end group have gained much interest,^{13,14} and that in the thin film state is worth studying. In this paper, the effect of the POSS as the chain end group on the viscosity and the glass transition temperature (T_g) of PS was examined. The structure of the PS-POSS thin films, which might be associated with the dewetting inhibition effect, was also investigated by the use of neutron reflectivity technique.

EXPERIMENTAL

Materials

TEMPO-based alkoxyamine with a hydroxy group^{15,16} was prepared as previously reported. 1-[Isocyanatopropyltrimethylsilyl]-3,5,7,9,11,13,15-heptacyclopentylpentacyclo[9.5.1.1^{3,9}.1^{5,15}.1^{7,13}]octasiloxane (POSS-NCO) was purchased from Aldrich Chemical Co. Styrene and deuterated styrene were purchased from commercial sources and purified by distillation under reduced pressure over calcium hydride. Polystyrene was purchased from Polymer Source, Inc. All other reagents were purchased from commercial sources and used as received. The silicon wafer substrates were purchased from Sumitomo Mitsubishi Silicon Co., and cleaned by immersion in the mixture of H₂SO₄ (97%) and H₂O₂ (34.5%) with volume ratio of 7:3 for 1 h at 353 K, rinsed in deionized water and dried under vacuum before spin-coating.

Measurements

¹H and ¹³C NMR spectra were recorded on a JEOL JNM-EX400 spectrometer using tetramethylsilane (TMS) as an internal standard in chloroform-*d* (CDCl₃). IR spectra were obtained with Perkin-Elmer Spectrum One infrared spectrometer. The number average molecular weight (M_n) and polydispersity (M_w/M_n) were estimated by gel permeation chromatographic (GPC) analysis. GPC measurement was carried out at 313 K on JASCO high performance liquid chromatography (HPLC) system equipped with a guard column (TOSOH TSKguardcolumn SuperH-L), three mixed columns (TOSOH TSKgel SuperH6000, 4000, and 2500), and a differential refractometer. Tetrahydrofuran (THF) was used as the eluent at a flow rate of 0.6 mL/min. Polystyrene standards ($M_n = 800$ –152000; $M_w/M_n = 1.03$ –1.10) were used to calibrate the GPC system.

Differential scanning calorimetry (DSC) was performed on DSC8230 (Rigaku) under nitrogen atmosphere at a heating rate of 10 K/min. Thermograms of the second heating process were stored and analyzed.

The rheological properties of the polymers were measured with a Physica MCR 101 (Anton Paar

GmbH). A parallel plate geometry with a diameter of 8 mm and a gap of 1 mm was used for all measurements. Samples were tested at temperatures between 383 and 423 K under nitrogen atmosphere with oscillation frequencies ranging from 100 to 0.1 rad/s and strain amplitude of 1%.

Neutron reflectivity (NR) measurements were performed using an Advanced Reflectometer for Interface and Surface Analysis (ARISA)¹⁷ on H5 beamline of Neutron Science Laboratory, High Energy Accelerator Research Organization. The theoretical NR was calculated using Parratt32 (version 1.5 HMI Berlin), and evaluated against the experimental data.

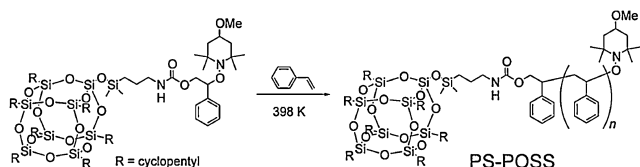
The static contact angles of 2 μ l droplets of deionized water and diiodomethane were measured using DSA-10 (Krüss Co., Ltd.). The surface free energies of the samples were calculated from the static contact angles using Owens and Wendt's method.¹⁸

Synthesis of POSS-containing Initiator

Catalytic amount of dibutyltin dilaurate was added to a dry toluene solution (3.5 mL) of the POSS-NCO (4.0 g, 3.8 mmol) and TEMPO-based alcohol (1.2 g, 3.8 mmol). The reaction mixture was stirred at room temperature under nitrogen atmosphere for 24 h. The crude product was purified by flash chromatography using an eluent of ethyl acetate/hexane/chloroform (1/3/12, v/v/v) and dried under vacuum to give the POSS-containing initiator as a white powder (3.2 g, 62% yield). ¹H NMR: δ /ppm 0.11 (s, 6H), 0.51 (m, 2H), 0.67 (s, 3H), 1.01 (m, 7H), 1.08 (s, 3H), 1.23 (s, 3H), 1.38 (s, 3H), 1.30–2.00 (m, 60H), 3.09 (m, 2H), 3.30 (s, 3H), 3.40 (m, 1H), 4.20 (dd, $J = 6$ Hz, 11 Hz, 1H), 4.56 (m, 1H), 4.63 (dd, $J = 6$ Hz, 11 Hz, 1H), 4.88 (t, $J = 6$ Hz, 1H), 7.20–7.40 (m, aromatic). FT-IR (KBr, cm⁻¹): 3100–2810, 1728 (C=O), 1522, 1452, 1252, 1200–1000, 913, 838, 757, 698, 505. FAB mass calculated for $[M + 1]^+$ C₅₉H₁₀₄N₂O₁₇Si₉, found 1365.

Polymerization

A mixture of the POSS-containing initiator (700 mg, 0.51 mmol) and styrene (1.5 mL, 13.1 mmol) was charged in a polymerization tube, degassed, and sealed off under vacuum. The mixture was incubated at 398 K for 24 h, and after dilution with chloroform the solution was poured into methanol. The precipitate was further purified by reprecipitation with a chloroform/methanol system and dried under vacuum to give the PS-POSS as a white powder (1.3 g, 63% yield). $M_n = 2500$, $M_w/M_n = 1.11$. ¹H NMR: δ /ppm 0.01–0.60 (br), 0.80–2.60 (br, aliphatic H), 3.03 (br), 3.2–4.5 (br), 6.20–7.40 (br, aromatic H). FT-IR (NaCl, cm⁻¹): 3100–2810, 1728 (C=O), 1602 (C=C), 1493, 1453, 1252, 1200–1000, 908, 838, 757, 698, 505.



Scheme 1. Synthesis of well-defined PS-POSS by NMRP.

Thin Film Preparation

Thin films were prepared by spin-coating the polymers dissolved in toluene, which had been passed through a PTFE filter (pore size = 0.20 μm), onto acid-cleaned silicon wafers at 2000 rpm for 30 s. The concentration of the polymer solution was 3 wt %. Under these conditions the films produced were approximately 110 nm thick as determined by ellipsometry using Imaging Ellipsometer (Moritex Corp.). Spin-coated films were annealed under vacuum at 393 K for 3 h and quenched to room temperature. Reflective optical images were obtained with an optical microscope, BX51 (Olympus Optical Co., Ltd.).

RESULTS AND DISCUSSION

Synthesis of PS-POSS

The synthesis of POSS-containing initiator was carried out by the addition reaction of POSS with an isocyanate pendant group to the TEMPO-based alkoxyamine with a hydroxy group. PS-POSS were prepared by NMRP using this initiator (Scheme 1). ^1H NMR detected a weak proton signal at 4.56 ppm attributed to the urethane linking groups, while a proton signal of the $-\text{CH}_2-\text{NCO}$ group at 3.27 ppm was disappeared. The structure of the initiator and PS-POSS was also confirmed by comparison of the Fourier transform infrared spectra of the two starting materials and the final product. After the addition reaction, the isocyanate absorption band at 2270 cm^{-1} of the starting material disappeared and the absorption corresponding to the stretching vibration of urethane carbonyl groups was observed at 1728 cm^{-1} . The synthesized PS-POSS showed the characteristic PS absorbance. These results concluded that the PS having a POSS at the chain end was successfully obtained.

Thermal Stability of PS-POSS Thin Film

Thermal stability of PS-POSS thin films was investigated. PS from commercial source with the almost same molecular weight as PS-POSS was used to make reference films. M_n and M_w/M_n of PS-POSS and PS were summarized in Table I. Optical micrographs of (a) 110 nm-thick PS2.1k ($M_n = 2100$, $M_w/M_n = 1.06$) and (b) 113 nm-thick PS-POSS2.5k ($M_n = 2500$, $M_w/M_n = 1.11$) thin films, after annealing, are shown in Figure 1. The bare substrate was observed

Table I. Summary of the molecular weight of PS and PS-POSS

Sample	M_n	M_w/M_n	POSS content (wt %)
PS2.1k	2100	1.06	0
PS44k	44000	1.04	0
PS-POSS2.5k	2500	1.11	36
PS-POSS43k	43000	1.11	2.1

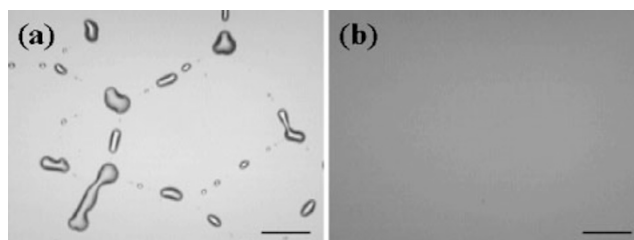


Figure 1. Optical micrographs of (a) PS2.1k and (b) PS-POSS2.5k thin films annealed at 393 K for 3 h. The length of the bar is 100 μm .

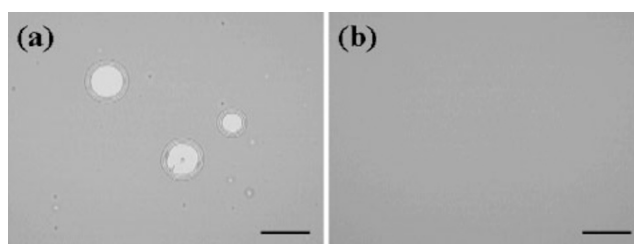


Figure 2. Optical micrographs of (a) PS44k and (b) PS-POSS43k thin films annealed at 393 K for 96 h. The length of the bar is 100 μm .

as a consequence of the complete dewetting of PS2.1k film, in contrast, no appreciable dewetting was observed in the PS-POSS2.5k film. This suggests that the introduction of POSS as a PS end group can inhibit the dewetting of the film. Interestingly, similar inhibition effect of dewetting was obtained for the PS-POSS43k ($M_n = 43000$, $M_w/M_n = 1.11$) film as shown in Figure 2, which contained less POSS fraction compared to the PS-POSS2.5k. The pure PS44k ($M_n = 44000$, $M_w/M_n = 1.04$) film broke up by the formation of holes, whereas PS-POSS43k film did not dewet at all.

Rheological Characterization of PS-POSS

To evaluate the effect of the bulk viscoelastic properties of PS-POSS on the dewetting inhibition, the rheological measurements were carried out. It is expected that the introduction of the POSS moiety into the end group of polymer chains affects the physical properties of the polymer dramatically, so the rheological characterization is important for comparing the viscoelastic behavior of the PS and PS-POSS systems.

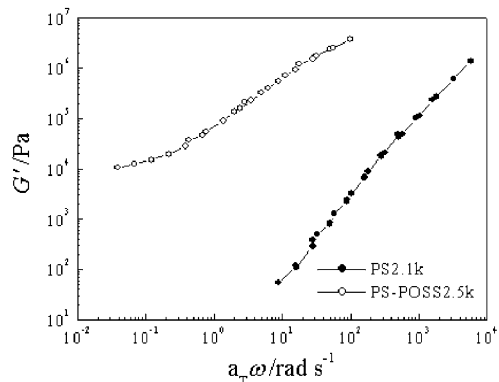


Figure 3. G' master curves of PS2.1k and PS-POSS2.5k at T_0 of 383 K.

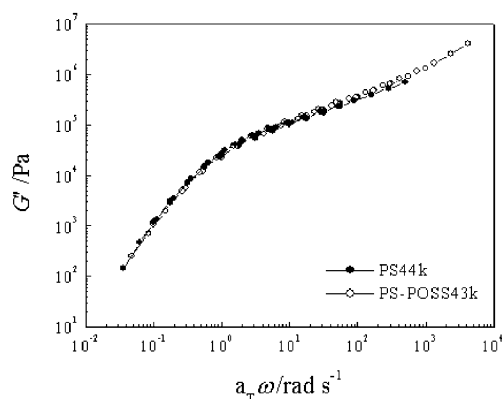


Figure 4. G' master curves of PS44k and PS-POSS43k at T_0 of 413 K.

Figures 3 and 4 illustrate the master curves of the storage modulus (G') for PS and PS-POSS. The master curves, generated by applying the principle of time-temperature superposition to isothermal frequency scans, were shifted to a reference temperature (T_0). The pure PS2.1k behaves as a Newtonian liquid with the viscoelastic properties exhibiting liquidlike characteristics, while PS-POSS2.5k exhibits pseudo-solid-like behavior as shown in Figure 3. The slope of G' vs. $a_T\omega$ at low frequency region of PS-POSS2.5k is approximately 0 in comparison to a typical slope of 2 for a Newtonian liquid. It was not possible to attain the terminal regime for the PS-POSS2.5k within the range of temperatures investigated and under the current experimental conditions. It is likely that the rheological behavior of PS-POSS2.5k is strongly influenced by the presence of POSS end groups. This may lead to dramatically altered diffusion of PS chains. On the other hand, PS-POSS43k exhibits the liquidlike characteristics as PS44k, and no influence of the POSS end group is observed as shown in Figure 4, because the relative weight fraction of POSS moiety in PS-POSS43k is much lower than that in PS-POSS2.5k.

Table II. The η_0 and T_g values of PS2.1k and PS-POSS2.5k

Sample	$\eta_0/\text{Pa}\cdot\text{s}$ ($T_0 = 383\text{ K}$)	T_g/K
PS2.1k	3.02×10^2	340
PS-POSS2.5k	7.81×10^5	348

Table III. The η_0 and T_g values of PS44k and PS-POSS43k

Sample	$\eta_0/\text{Pa}\cdot\text{s}$ ($T_0 = 413\text{ K}$)	T_g/K
PS44k	6.74×10^4	375
PS-POSS43k	7.25×10^4	375

Zero-shear-rate viscosities (η_0) were calculated and reported in Table II with the T_g values obtained from DSC for PS2.1k and PS-POSS2.5k. The η_0 and T_g of PS-POSS2.5k were higher than those of the pure PS2.1k, indicating that the massive POSS inorganic end groups strongly restricted the PS chain motion. The dewetting of a polymer film from a substrate has been observed to proceed with a velocity inversely proportional to the bulk viscosity of the dewetting fluid.¹⁹ It was assumed that the increase of the viscosity contributed to the inhibition of the dewetting in the low molecular weight region.

Table III summarized the η_0 and T_g values of PS44k and PS-POSS43k. Comparison of Table II and Table III shows the influence of chain length on the rheological properties of the PS-POSS. There was no noticeable difference in the η_0 and T_g values of PS44k and PS-POSS43k because of the decrease in the relative weight fraction of POSS moiety to PS by the increase of PS chain length. However, PS-POSS43k gave rise to dewetting inhibition, as shown in Figure 2, suggesting the existence of some other factors attributing the film stabilization effect.

Structure of PS-POSS Thin Films

To understand the origin of this dewetting inhibition, NR measurement was applied to examine the depth composition profile of the deuterated PS-POSS (dPS-POSS) thin film. dPS-POSS was prepared by NMRP of deuterated styrene using POSS-containing initiator, as the same procedure of PS-POSS. Since the neutron scattering length density (b/V), of the dPS chain is much larger than that of the POSS moiety, the dispersion state of the POSS end groups in the PS-POSS film can be detected. The intensity of the reflected neutron beam was recorded as a function of the scattering vector ($q = 4\pi \sin\theta/\lambda$). Figure 5 shows the reflectivity profile of dPS-POSS8.2k ($M_n = 8200$, $M_w/M_n = 1.07$) thin film. The solid line is the fit of the reflectivity profile and inset shows b/V profile used to generate the fit. The horizontal axis of the inset corresponds to the distance perpendicular to the film.

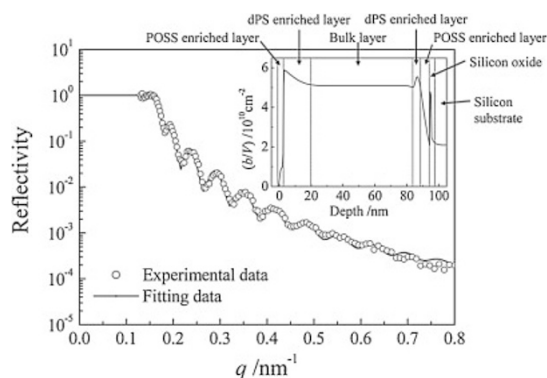


Figure 5. NR data from dPS-POSS8.2k thin film annealed at 393 K for 2 h. The inset shows the b/V profile used to calculate the reflectivity profiles as the solid line.

The data were fit with a seven-layer model as shown in the inset of Figure 5. The first layer is the film surface with lower b/V than that of the bulk region in middle part of the film because of the segregation of the POSS moieties of dPS-POSS. The second layer with high b/V between POSS enriched layers and the bulk region is due to the localization of dPS chains connected to the POSS end groups segregated to the surface. The third layer is the bulk region having the b/V value of the mixture of a dPS chain and a POSS end group. It can be seen that the POSS moieties is located at the interface between the film and substrate, as well as the film surface. The fourth layer is the dPS-rich layer, and at the fifth layer, substrate interface, the decrease of the b/V by the segregation of POSS moieties is observed. The sixth and seventh layers are the silicon oxide on the substrate and silicon substrate itself, respectively. This result suggests the existence of the enrichment layer of POSS end groups at the surface and film–substrate interface of the dPS-POSS thin film.

POSS Enrichment at the Interfaces of PS-POSS Thin Films

The segregation of the POSS end groups to the film surface might be due to the difference of the surface free energy between PS chain and POSS moiety, and can be expected to affect the surface free energy of the PS films. Surface energetics is an important factor causing the film rupture, and the key to whether a film is stable or not on a certain substrate is given by Young's equation, which is the criteria for spreading, as the spreading coefficient (S),²⁰

$$S = \gamma_B - (\gamma_A + \gamma_{AB}) \quad (1)$$

where γ_A and γ_B are the surface free energies of the polymer film and substrate, respectively, and γ_{AB} is the free energy of the film–substrate interface. If S

Table IV. Contact angles, surface free energies, and S of PS44k and PS-POSS43k thin films

Sample	$\theta_{\text{H}_2\text{O}}$ /deg.	$\theta_{\text{CH}_2\text{I}_2}$ /deg.	γ^d /mJ·m ⁻²	γ^h /mJ·m ⁻²	γ /mJ·m ⁻²	S /mJ·m ⁻²
PS44k	97.9	23.9	48.06	0.02	48.08	-20.8
PS-POSS43k	93.3	20.3	48.36	0.07	48.43	-19.7
Si substrate	19.4	40.7	28.1	41.4	69.5	—

is negative, then the film is unstable. The introduction of the low energy end group to a polymer was reported to inhibit the dewetting process of the polymer thin film by the reduction of the surface free energy of the film.²¹ To understand the effect of S on the inhibition of the dewetting in PS-POSS films, the surface free energies of the PS44k film, PS-POSS43k film and Si substrate were estimated by the static contact angle measurements of water and diiodomethane. The surface free energy, γ , and its dispersive and hydrogen-bonding components, γ^d and γ^h , respectively, were calculated from the static contact angles using Owens and Wendt's equation.¹⁸ The interfacial free energy of the film and acid-cleaned Si substrate, γ_{AB} , was evaluated using the extended Fowkes equation.¹⁸ The values of the contact angles (θ) and free energies are shown in Table IV. S of the films on the substrate was evaluated from the surface energies shown in Table IV. The noticeable difference in the surface free energy between PS44k and PS-POSS43k was not observed. Both of the PS44k film and the PS-POSS43k film had the negative S , indicating the inhibition of the dewetting was occurred from the other factors.

The results mentioned above insisted that the inhibition of dewetting in PS-POSS thin film is closely related to the segregation of POSS end groups to the film–substrate interface. The driving force of the enrichment of POSS end groups at the interface has not been proved yet, however, the less unfavorableness of the interaction between POSS moiety and Si substrate than that between PS chain and the substrate seems to cause the segregation of POSS end group to the interface. The dewetting inhibition effects of the end-functionalized polymer films by the immobilization of the end group on the inorganic substrate were reported using specialized end groups with high affinity for the substrate like ionic groups and metal complex,^{3,4} and this paper shows the potential use of the nanofiller like POSS as a kind of the end group for the tethering of polymer chain onto the substrate. The enrichment of POSS moieties at film–substrate interface can act as a tether of the chains, and entanglements between the tethered and untethered PS-POSS chains seem to prevent the dewetting of the whole film.

Acknowledgment. The present work was partially supported by a Grant-in-Aid for Scientific Research from the Ministry of Education, Culture, Science, Sports and Technology of Japan. The present work is also supported by a Grant-in-Aid for the Global COE Program, "Science for Future Molecular Systems" from the Ministry of Education, Culture, Science, Sports and Technology of Japan. N. H. acknowledges the financial support of Grant-in-Aid for JSPS Fellows.

REFERENCES

1. G. Reiter, *Langmuir*, **9**, 1344 (1993).
2. R. R. Netz and D. Andelman, *Phys. Rev. E*, **55**, 687 (1997).
3. R. Yerushalmi-Rozen, J. Klein, and L. J. Fetters, *Science*, **263**, 793 (1994).
4. G. Henn, D. G. Bucknall, M. Stamm, P. Vanhoorne, and R. Jerome, *Macromolecules*, **29**, 4305 (1996).
5. K. A. Barnes, A. Karim, J. F. Douglas, A. I. Nakatani, H. Gruell, and E. J. Amis, *Macromolecules*, **33**, 4177 (2000).
6. N. Hosaka, K. Tanaka, H. Otsuka, and A. Takahara, *Compos. Interfaces*, **11**, 297 (2004).
7. T. S. Haddad and J. D. Lichtenhan, *Macromolecules*, **29**, 7302 (1996).
8. K. M. Kim, D. K. Keum, and Y. Chujo, *Macromolecules*, **36**, 867 (2003).
9. K. Koh, S. Sugiyama, T. Morinaga, K. Ohno, Y. Tsujii, T. Fukuda, M. Yamahiro, T. Iijima, H. Oikawa, K. Watanabe, and T. Miyashita, *Macromolecules*, **38**, 1264 (2005).
10. N. Hosaka, N. Torikai, H. Otsuka, and A. Takahara, *Langmuir*, **23**, 902 (2007).
11. K. Miyamoto, N. Hosaka, H. Otsuka, and A. Takahara, *Chem. Lett.*, **35**, 1098 (2006).
12. C. J. Hawker, A. W. Bosman, and E. Harth, *Chem. Rev.*, **101**, 3661 (2001).
13. X. Wang and Y.-Y. Yan, *Polymer*, **47**, 6267 (2006).
14. K. Ohno, S. Sugiyama, K. Koh, Y. Tsujii, T. Fukuda, M. Yamahiro, H. Oikawa, Y. Yamamoto, N. Ootake, and K. Watanabe, *Macromolecules*, **37**, 8517 (2004).
15. C. J. Hawker, G. G. Barclay, and J. Dao, *J. Am. Chem. Soc.*, **118**, 11467 (1996).
16. R. Matsuno, K. Yamamoto, H. Otsuka, and A. Takahara, *Macromolecules*, **37**, 2203 (2004).
17. N. Torikai, M. Furusaka, H. Matsuoka, Y. Matsushita, M. Shibayama, A. Takahara, M. Takeda, S. Tasaki, and H. Yamaoka, *Appl. Phys. A*, **74** (Suppl.), S264 (2002).
18. D. K. Owens and R. C. Wendt, *J. Appl. Polym. Sci.*, **13**, 741 (1969).
19. C. Redon, F. Brochard-Wyart, and F. Rondelez, *Phys. Rev. Lett.*, **66**, 715 (1991).
20. A. W. Adamson, in "Physical Chemistry of Surface," 5th ed., Wiley, New York, 1990; Chapter 10.
21. C. Yuan, M. Ouyang, and J. T. Koberstein, *Macromolecules*, **32**, 2329 (1999).